Molecular Cell
Article

Transcriptome-wide miR-155 Binding Map Reveals Widespread Noncanonical MicroRNA Targeting

Gabriel B. Loeb,[1,2,7] Aly A. Khan,[3,4,7] David Canner,[1,2] Joseph B. Hiatt,[5] Jay Shendure,[5] Robert B. Darnell,[6] Christina S. Leslie,[3] and Alexander Y. Rudensky[1,2,*]
[1]Howard Hughes Medical Institute
[2]Immunology Program
[3]Computational Biology Program
Memorial Sloan-Kettering Cancer Center, New York, NY 10065, USA
[4]Institute for Genomics and Systems Biology, University of Chicago, Chicago, IL 60637, USA
[5]Department of Genome Sciences, University of Washington, Seattle, WA 98195, USA
[6]Howard Hughes Medical Institute, Laboratory of Molecular Neuro-Oncology, The Rockefeller University, New York, NY 10065, USA
[7]These authors contributed equally to this work
*Correspondence: rudenska@mskcc.org
http://dx.doi.org/10.1016/j.molcel.2012.10.002

SUMMARY

MicroRNAs (miRNAs) are essential components of gene regulation, but identification of miRNA targets remains a major challenge. Most target prediction and discovery relies on perfect complementarity of the miRNA seed to the 3′ untranslated region (UTR). However, it is unclear to what extent miRNAs target sites without seed matches. Here, we performed a transcriptome-wide identification of the endogenous targets of a single miRNA—miR-155—in a genetically controlled manner. We found that approximately 40% of miR-155-dependent Argonaute binding occurs at sites without perfect seed matches. The majority of these noncanonical sites feature extensive complementarity to the miRNA seed with one mismatch. These noncanonical sites confer regulation of gene expression, albeit less potently than canonical sites. Thus, noncanonical miRNA binding sites are widespread, often contain seed-like motifs, and can regulate gene expression, generating a continuum of targeting and regulation.

INTRODUCTION

MicroRNAs (miRNAs) direct Argonaute (AGO) proteins to post-transcriptionally repress messenger RNA (mRNA) targets and regulate a broad range of physiological processes (Ambros, 2004; Bartel, 2004, 2009). While gain- and loss-of-function studies have established specific roles of individual miRNAs, the identity of most miRNA targets remains unknown, which limits mechanistic insight into observed phenotypes. For instance, it is unclear whether individual miRNAs target multiple components of the same regulatory pathway, individual components of related pathways, or multiple unrelated pathways.

Early studies using both reporter assays and analysis of down-regulated genes in miRNA overexpression experiments revealed that perfect complementarity of the 5′ end of the miRNA (i.e., the "seed" region at positions 2–7) to the 3′ untranslated region (UTR) of target RNAs is the most common determinant of target specificity (Brennecke et al., 2005; Doench and Sharp, 2004; Lewis et al., 2003, 2005; Lim et al., 2005). However, many reports suggest regulation of sites without perfect seed complementarity (Betel et al., 2010; Brennecke et al., 2005; Didiano and Hobert, 2006; Lal et al., 2009; Lu et al., 2010; Shin et al., 2010; Vella et al., 2004; Vo et al., 2010). Recently, biochemical identification of AGO binding sites became possible with high-throughput sequencing of RNA isolated by crosslinking immunoprecipitation (HITS-CLIP) and photoactivatable-ribonucleoside-enhanced crosslinking and immunoprecipitation (PAR-CLIP) techniques, which combine RNase treatment and AGO immunoprecipitation with high-throughput sequencing to identify sites of AGO binding across the transcriptome (Chi et al., 2009; Gottwein et al., 2011; Hafner et al., 2010; Leung et al., 2011; Skalsky et al., 2012; Zisoulis et al., 2010). In these studies, a sizable fraction of CLIP-identified AGO binding sites did not contain seed matches. However, it was unclear whether the majority of this apparently seedless targeting was caused by miRNA independent mechanisms (Leung et al., 2011) or by noncanonical miRNA-target interactions. Thus, the mechanism and gene regulatory potential of these seedless interactions remained in question.

To address miRNA dependent targeting by AGO without reliance on sequence motifs, we combined genetic, biochemical, and computational approaches. We analyzed binding sites using differential HITS-CLIP (dCLIP) and mRNA expression changes in primary cells isolated from mice that are wild-type or deficient for a single miRNA. We used miR-155 as a model for the following reasons: miR-155 knockout mice show a marked impairment in T and B cell function (Rodriguez et al., 2007; Thai et al., 2007; Vigorito et al., 2007), miR-155 is highly expressed in human malignancies (Eis et al., 2005; Kluiver et al., 2005; Metzler et al., 2004; Volinia et al., 2006), and its overexpression in pre-B cells (Costinean et al., 2006) or hematopoietic stem cells (O'Connell et al., 2008) leads to oncogenic transformation. Importantly, miR-155 is abundant in activated T cells, whereas naive wild-type T cells are devoid of miR-155 and are therefore similar to miR-155-deficient counterparts. Thus, we employed AGO dCLIP to identify miR-155-dependent binding sites using wild-type

(WT) and miR-155-deficient (155KO) primary T cells. Our analysis of differential AGO binding confirmed that exact complementarity to nucleotides 2–7 of the miRNA is present in the majority of miR-155-dependent binding sites. We also found that perfect seed matches are absent in ~40% of miR-155-dependent AGO binding sites. These noncanonical sites, which are undetectable by seed-based miRNA target prediction algorithms, were strongly enriched for inexact seed matches, which contained a mismatch to the seed at a single nucleotide position. Furthermore, noncanonical miRNA binding sites regulate gene expression, albeit less potently than canonical sites.

In contrast to seed matches in the 3′ UTR, differential gene expression analysis after miRNA perturbation indicated that, as a group, seed matches within coding regions have little gene regulatory activity (Grimson et al., 2007; Lim et al., 2005). Previous studies using CLIP techniques demonstrated extensive AGO binding to the coding region, although these sites were observed to mediate less regulation than 3′ UTR sites (Chi et al., 2009; Gottwein et al., 2011; Hafner et al., 2010; Leung et al., 2011; Skalsky et al., 2012; Zisoulis et al., 2010). However, several groups reported features that lead to more regulation by sites in the coding region (Fang and Rajewsky, 2011; Forman et al., 2008; Gu et al., 2009; Schnall-Levin et al., 2011). For this reason, we investigated whether sites with stringently defined Argonaute binding to coding regions lead to functional gene regulation. Using AGO dCLIP, we showed miR-155-dependent AGO binding to a subset of miR-155 seed matches within coding regions. However, these sites did not lead to detectable downregulation of steady state mRNA levels, leaving open the possibility that these sites may have other functions.

Our AGO dCLIP analysis identified, in a genetically controlled manner, a transcriptome-wide set of direct targets for a miRNA in a specific cellular context and revealed the unexpected prevalence of noncanonical targeting by miRNAs.

RESULTS

Analysis of AGO Binding Sites in miR-155-Sufficient and -Deficient T Cells

Although barely detectable in naive T cells, miR-155 was dramatically upregulated upon activation of $CD4^+$ T cells induced by TCR and costimulatory receptor CD28 ligation (Figure S1A available online). In order to reveal miR-155-dependent binding of AGO in primary T cells, we performed AGO dCLIP using activated $CD4^+$ T cells isolated from WT and miR-155 KO C57Bl/6 mice. We UV crosslinked protein-mRNA complexes in the activated T cells and followed with partial RNase digestion and stringent immunoprecipitation with an anti-Argonaute 2 antibody. The published AGO HITS-CLIP protocol (Chi et al., 2009) was modified to increase coverage and dynamic range and to reduce sequencing costs (see the Experimental Procedures).

Libraries constructed from 12 biological replicates of activated 155KO and WT $CD4^+$ T cells were subjected to high-throughput sequencing, and the reads that uniquely aligned to the annotated 3′ UTR sequences of the mouse genome were analyzed (a total of 5,213,578 and 5,334,757 uniquely mapping reads from WT and 155KO libraries, respectively) (Figure 1A; see the Supplemental Experimental Procedures). To detect AGO binding sites, we developed a peak calling algorithm based on edge detection (see the Supplemental Experimental Procedures). This algorithm was essential for identifying overlapping binding sites (Figures S2B–S2D) and is effective for binding site detection in other data sets (Figure S2E).

In T cells, we identified 14,634 reproducible AGO binding sites in the 3′ UTRs of 4,165 genes (Table S1 and http://cbio.mskcc.org/leslielab/clipseq/). We limited our analysis to these sites, which contained reads mapped from at least seven of the 12 replicates in either WT or 155KO T cell libraries.

Additional analyses confirmed that the observed changes in AGO binding were a direct effect of miR-155 deficiency. First, principal component analysis revealed that the transcriptomes of 155KO and WT activated T cells were very similar (Figure S1B). Second, AGO dCLIP libraries from 155KO cells, which included miRNAs, showed no changes in AGO-bound miRNA levels other than miR-155 itself (Figure S1C). Therefore, miR-155 loss did not cause major changes in the activation state, miRNA expression, or global transcriptome of activated T cells at the time point of analysis.

To validate AGO dCLIP, we examined 3′ UTR AGO binding sites containing miR-155 seed matches. We expected these seed match sites to exhibit more AGO binding in WT cells than 155KO cells (Figure 1B). Indeed, for the vast majority of the known targets of miR-155 (Bolisetty et al., 2009; Costinean et al., 2009; Levati et al., 2011; O'Connell et al., 2008, 2009; Rai et al., 2010; Wang et al., 2011), we observed differential AGO binding at miR-155 seed matches. Using this approach, we identified many targets, including PDL1, the ligand for the key inhibitory receptor PD1. Analysis of all AGO sites containing miR-155 seed matches showed that they had significantly reduced binding in 155KO cells compared to all AGO binding sites ($p < 4 \times 10^{-74}$) (Figure 1C). The observed differential binding at canonical miR-155 targets confirms that AGO dCLIP detects miR-155-dependent binding sites.

We used a stringent statistical test to discern miR-155-dependent sites from other AGO binding sites. At 191 AGO binding sites in 175 genes, there was significantly more AGO binding in WT than 155KO cells (cutoff at $p < 0.01$; see the Supplemental Experimental Procedures and Table S2). We next investigated whether differential AGO binding correlated with greater target regulation of AGO binding sites containing miR-155 seed matches (57% of all miR-155-dependent sites). Specifically, we compared expression changes in 155KO T cells for genes with AGO binding at miR-155 seed matches against the subset of genes with significant differential AGO binding at miR-155 seed matches (Figure 1D). As expected, we found stronger regulation of target genes with differential AGO binding at miR-155 seed matches. To quantitatively examine whether differential AGO binding is associated with greater gene regulation at AGO-bound miR-155 seed matches, we performed a linear regression analysis, which showed that differential AGO binding at sites with miR-155 seed matches correlated with downregulation ($p < 0.05$) (Figure S2F). Nearly all (>87%) AGO binding sites containing miR-155 seed matches had less binding in 155KO cells than in WT cells (using a normalized read count difference of 0). Furthermore, genes with AGO-bound miR-155 seed matches were greatly induced relative to genes with miR-155

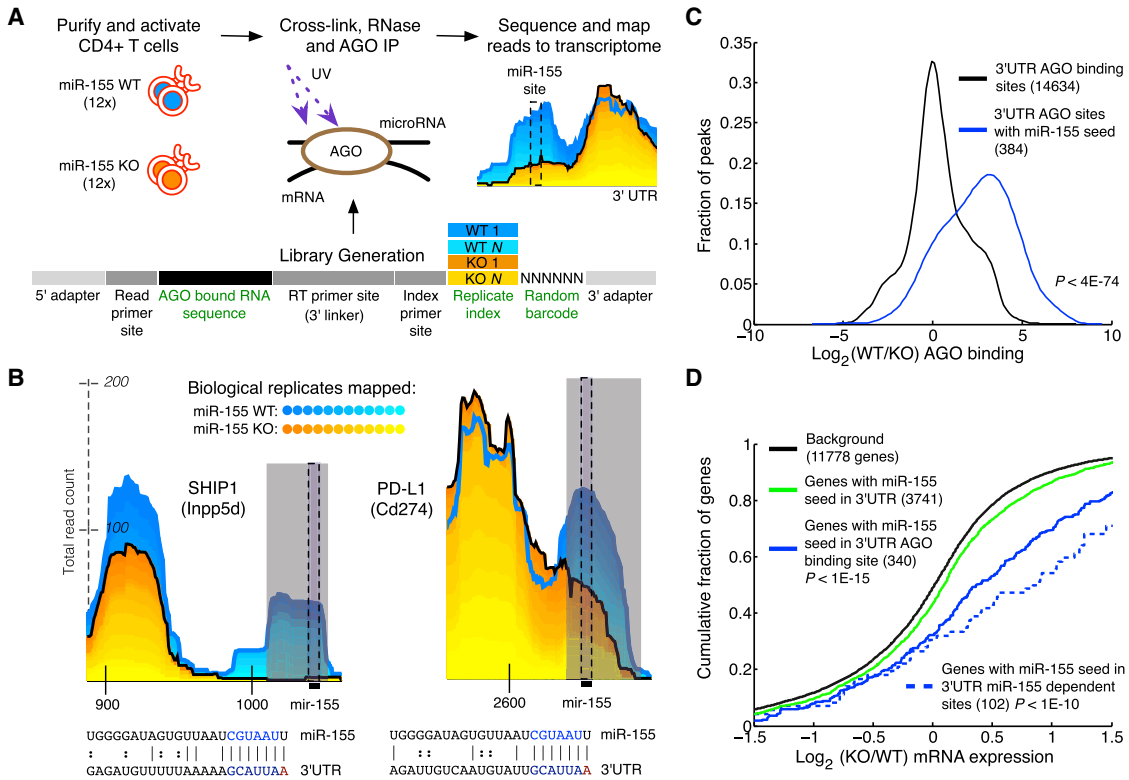

Figure 1. Differential CLIP-Sequencing Identifies Sites of miR-155-Mediated Argonaute Binding

(A) CD4$^+$ T cells were isolated from miR-155-sufficient and -deficient mice and RNase-treated cell lysates were subjected to Argonaute (AGO) immunoprecipitation. After stringent purification of complexes, indexed and barcoded libraries were prepared and subjected to Illumina high-throughput sequencing.

(B) Examples of canonical AGO binding sites in *PD-L1* and the previously described target *SHIP1*. Grey rectangles indicate miR-155-dependent binding sites ($p < 0.01$) called by edge-detection method. Reads from the 12 replicates have been stacked; blue shades are miR-155-sufficient (WT) replicates, and yellow shades are mir-155-deficient (155KO) replicates. Black bars indicate the location of the miR-155 seed in the binding site. Coordinates along the x axis indicate nucleotide position relative to the beginning of the 3′ UTR. The y axis indicates read counts, which are square root transformed after individual library normalization (see the Supplemental Experimental Procedures).

(C) Relative AGO binding in WT and 155KO cells at all 3′ UTR binding sites or 3′ UTR binding sites containing a miR-155 seed.

(D) Gene expression differences assessed by microarray between WT and 155KO cells of targets predicted by seed, AGO binding sites, or miR-155-dependent AGO binding sites.

p values were calculated with a one-sided KS test. See also Figure S1 and Table S1.

seed matches at which no AGO binding is detected (Figure 1D). Together, these data indicate that dCLIP improves the specificity of CLIP, yet for highly expressed miRNAs, the presence of a miRNA seed match within an AGO binding site usually identifies a miRNA target.

Analysis of AGO Binding Sites Outside the 3′ UTR

In addition to the prevalent binding that occurs in the 3′ UTR, we observed reads mapping to other transcribed regions including the 5′ UTR, coding regions, and the introns of genes (Figure 2A). Closer inspection revealed that most intronic reads were unclustered or mapped to small nucleolar RNAs (snoRNAs). AGO binding to snoRNAs was previously described (Ender et al., 2008; Saraiya and Wang, 2008; Taft et al., 2009), and our experiments provide further data concerning AGO binding to transcripts generated by snoRNA loci in mammals.

To determine whether AGO bound coding region sites in a miRNA-dependent fashion, we examined sites with miR-155 seed matches. Examining binding sites observed in at least seven of 12 replicates, we observed 137 AGO binding sites containing miR-155 seed matches in the coding regions of 129 genes. Many of these sites had clear miR-155-dependent binding (Figure 2B). Indeed, AGO binding at miR-155 seed matches in the coding region and the 3′ UTR was similarly miR-155 dependent (Figure 2C), although there were almost three times as many sites in the 3′ UTR. This miR-155 dependence confirms that AGO-miRNA complexes bind to the coding region.

Rare codons 5′ of miRNA complementary sites in the coding region contribute to more effective miRNA-mediated regulation (Gu et al., 2009). Consistent with this observation, PAR-CLIP revealed that AGO binding occurs at sites flanked by sequences enriched for rare codons (Hafner et al., 2010). Our data confirm this observation (Figure S3). Surprisingly, as was seen in the previous study of AGO binding, rare codons appeared to be more common both 5′ and 3′ of AGO binding sites.

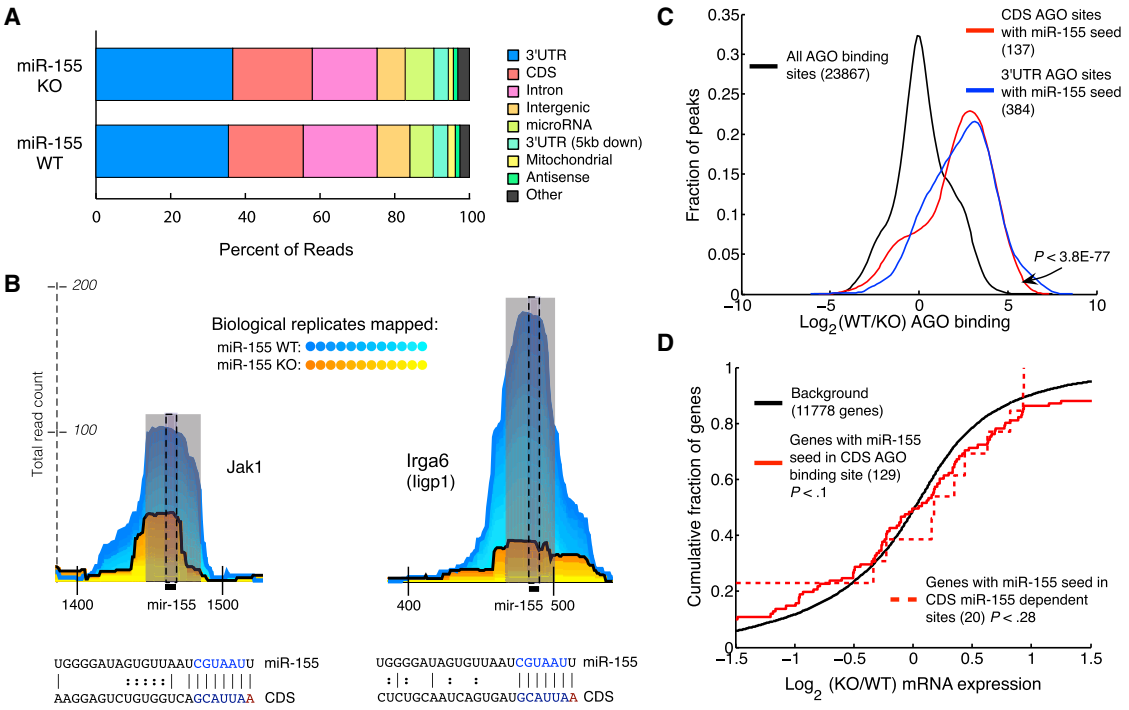

Figure 2. Argonaute Binding to Coding Regions

(A) Proportion of reads from miR-155-sufficient (WT) and miR-155-deficient (155KO) libraries mapping to various regions of the genome.

(B) Examples of AGO binding sites in the coding region. Coordinates along the x axis indicate nucleotide position relative to the beginning of the transcript.

(C) Relative AGO binding in WT and 155KO cells at all binding sites, 3′ UTR binding sites containing a miR-155 seed, or CDS binding sites containing a miR-155 seed.

(D) Gene expression differences assessed by microarray between WT and 155KO cells of targets predicted by AGO binding sites in the coding region.

p values were calculated with a one-sided KS test. See also Figures S2 and S3.

We applied the same stringent statistical test for miR-155 dependence that we applied to 3′ UTR sites. This identified 20 genes with sites in the coding region that contained a miR-155 seed and displayed significant miR-155 dependence. However, in contrast to 3′ UTR site-containing mRNAs, these mRNAs were not regulated by miR-155 (Figure 2D). Therefore, although miR-155 AGO complexes bound the coding region, this binding was not sufficient for transcript regulation.

Identification of Noncanonical AGO Binding Sites with AGO dCLIP

The strength of AGO dCLIP is the ability to identify miRNA-dependent binding sites without reliance on seed matches. We found that 34% of 3′ UTR AGO binding sites did not have a seed match for any of the 40 highest expressed miRNAs in our cells (Figure 3A), in agreement with previous reports (Chi et al., 2009; Hafner et al., 2010; Zisoulis et al., 2010). These 40 miRNAs represented more than 75% of the reads mapped to miRNA genes in libraries isolated from WT and 155KO cells (Figure S4). Of these miRNAs, the lowest expressed miRNA had less than 1% of the reads of the highest expressed miRNA. Accounting for AGO binding sites with this many seeds probably overestimates the amount of seed-mediated targeting.

Recent work in embryonic stem cells (ESCs) suggested that there are miRNA-independent G-rich motifs associated with AGO binding sites (Leung et al., 2011); however, these motifs were found in less than 2% of AGO binding sites identified in activated T cells. These results suggested that "noncanonical" miRNA dependent targeting is common.

We next focused on miR-155-dependent AGO binding sites in 3′ UTRs. While the majority of these sites contained miR-155 seed matches, ~43% did not (Figure 3A and Table S3). Increase of the stringency for miR-155 dependence ($p < 0.005$) did not substantially alter this percentage of seedless sites (~37%). These candidate noncanonical sites without a miR-155 seed, but with significantly more AGO binding in WT than in 155KO T cells, were found within genes with (e.g., *Hif1a* and *Trib1*) and without (e.g., *Unc119b*, *Cep135*, and *Gimap3*) miR-155 canonical sites (Figures 3B and 3C).

To determine whether miR-155 binds these noncanonical sites directly, we first looked for complementarity to the miR-155 sequence. We implemented a supervised learning strategy to optimize parameters for miR-155/AGO binding site alignments to discriminate between miR-155-dependent binding sites and -independent AGO binding sites (see the Supplemental Experimental Procedures). The optimized parameters rely on extensive complementarity to the seed region of miR-155 to discriminate more than 75% of miR-155-dependent binding sites from nondifferential AGO binding sites (average of 10-fold coefficient of variation; see the Supplemental

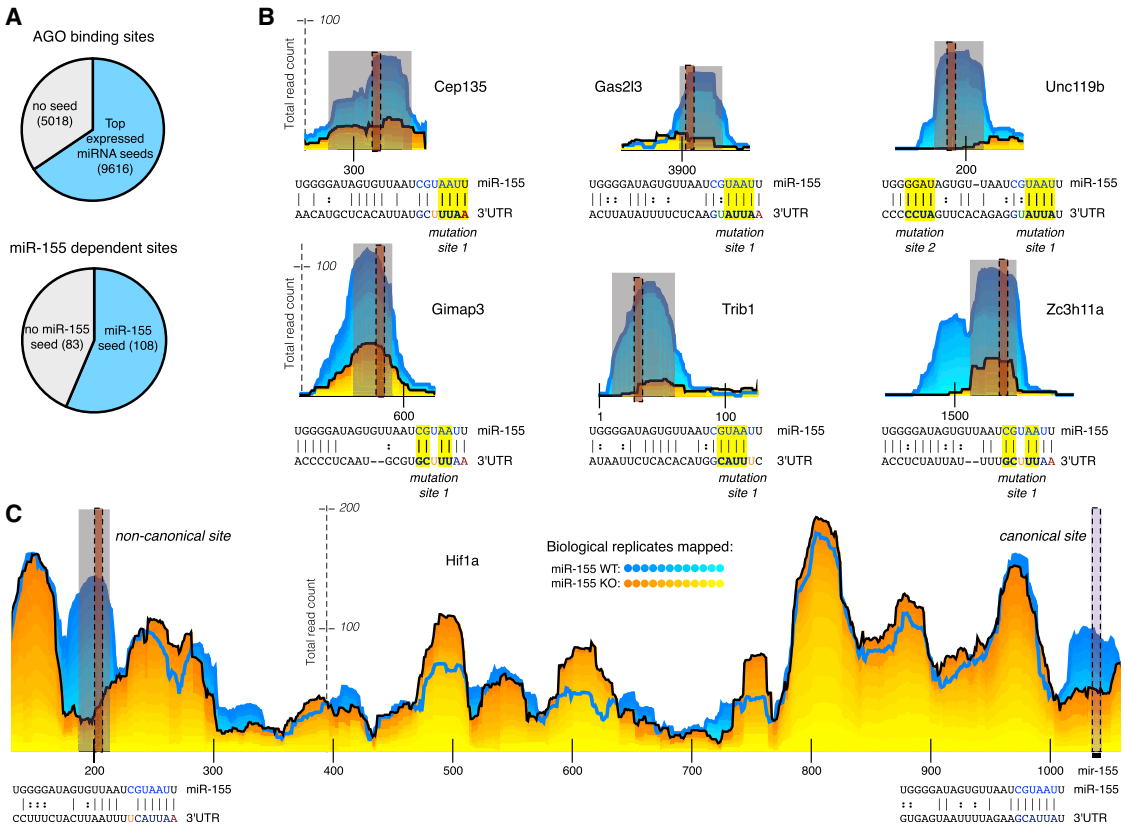

Figure 3. Many miRNA-Dependent Sites Do Not Contain Seed Matches

(A) Proportion of sites from all AGO binding sites or from miR-155-dependent sites that do not contain seed matches.

(B) Examples of noncanonical targets. Red vertical lines indicate the location of a seed-like motif in the site. Predicted base pairing between miR-155 and 3′ UTR sequences is indicated below AGO dCLIP read distribution profiles. Positions selected for mutations in luciferase reporter constructs are highlighted in the alignment.

(C) Example of a gene with both a noncanonical and a canonical site in the same 3′ UTR; numbers along the horizontal axis indicate nucleotides from the start of the 3′ UTR.

See also Figure S4, Table S2, and Table S3.

Experimental Procedures). To identify global patterns in the alignments between miR-155 and miR-155-dependent AGO binding sites, we grouped the alignments based on complementarity to the seed region. The most frequent motifs were represented by sequences with exact complementarity to nucleotides 1–7 (for miR-155, this includes an A at position 1) and nucleotides 1–8. This group of motifs was followed by sequences with complementarity to nucleotides 2–8, and with complementarity to nucleotides 2–7 (Figure 4A). However, in addition to these expected canonical motifs, we found several types of seed-like motifs that, to the best of our knowledge, have not been previously described at a transcriptome-wide level. These included motifs with inexact complementarity to the miR-155 seed such as mismatches at positions 5 and 7 and a G:U wobble at position 6 (Figure 4A). The observed complementarity for miR-155 within noncanonical AGO binding sites implied that AGO dCLIP specifically identified sites of direct miR-155 targeting.

We next investigated whether these seed-like motifs were able to mediate in vivo interactions with miR-155-loaded AGO complexes. Previous work showed that a small percentage of HITS-CLIP reads contain deletions, which are likely a consequence of reverse transcription errors at sites of UV-induced protein-RNA crosslinking (Zhang and Darnell, 2011). Because UV-mediated crosslinking was preformed on live cells, deletions within binding sites are evidence of in vivo interactions. We mapped deletions surrounding sites of miR-155 canonical motifs and found a large number of deletions proximal to miR-155 seed matches in libraries generated from WT but not 155KO T cells (Figure 4B). As expected, deletions proximal to miR-21 seeds were found equally in WT and 155KO libraries. To assess frequencies of deletions at noncanonical miR-155-dependent AGO binding sites, we used the seed-like motifs identified by our supervised learning algorithm. We found many deletions in WT but not in 155KO libraries near seed-like motifs in noncanonical sites. This result indicated that our sequence alignment strategy effectively identified the site of miR-155 interaction within AGO-bound regions and demonstrated that the interaction between miR-155 and noncanonical sites occurs in vivo.

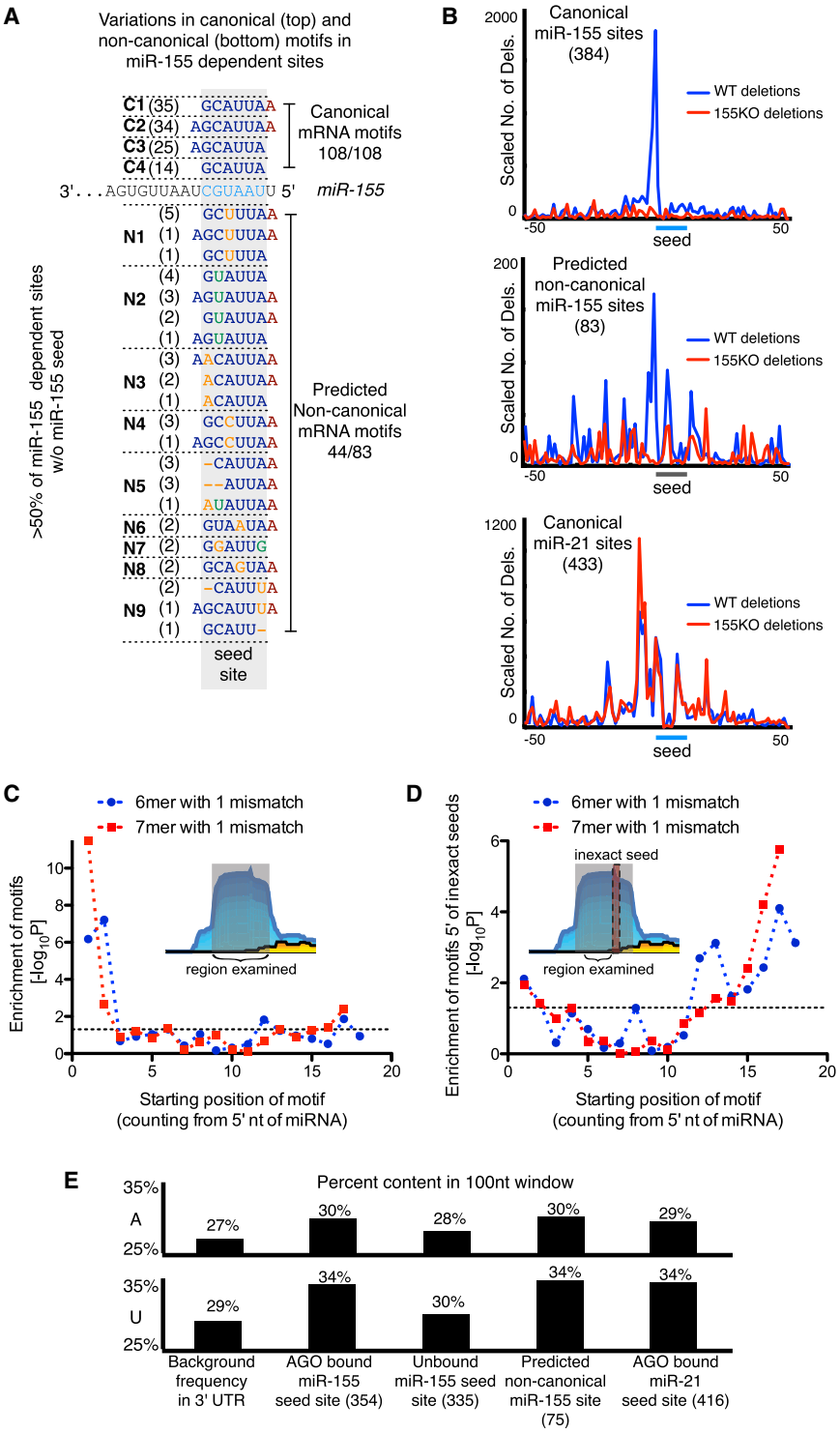

Figure 4. Characteristics of Noncanonical Sites

(A) Variations in canonical (top) and noncanonical (bottom) motifs in miR-155-dependent sites. Numbers in parentheses indicate the number of miR-155-dependent AGO binding sites containing the motif.

(B) Crosslinking-induced deletions around canonical seed matches and noncanonical seed-like motifs.

(C) Enrichment for inexact 6-mer and 7-mer motifs in noncanonical miR-155-dependent ($p < 0.01$) sites relative to all binding sites.

(D) Enrichment of 3′ complementarity in noncanonical miR-155 binding sites. Enrichment of motifs complementary to miR-155 was examined in 16 nt regions found 3–18 nt 5′ of inexact seed matches in noncanonical miR-155-dependent ($p < 0.05$) sites relative to equally sized regions in Argonaute binding sites lacking miR-155 seed matches. Enrichments were calculated with Fisher's Exact Test.

(E) AU content in a 100 nt window centered at seed matches or noncanonical seed-like motifs. See also Figures S5 and S8.

Features of Noncanonical miR-155 Binding Sites

Further insights into noncanonical sites came from focused analysis of seedless miR-155-dependent binding sites. These sites exhibited a strong enrichment for seed region motifs that contained a single mismatch from the miRNA seed (up to $p < 10^{-10}$ for the inexact 7-mer from nucleotides 1–7) (Figure 4C). A subtle enrichment ($p < 0.05$) for inexact matches to the 3′ end of the miRNA was also apparent. We examined whether noncanonical sites contained sequences complementary to the 3′ end of the miRNA by focusing on sequences 5′ of motifs with a single mismatch from a miR-155 seed, where supplementary 3′ binding is expected to occur. These subregions showed strong enrichment for complementarity to the 3′ end of miR-155 (from $p < 0.03$ to $p < 10^{-5}$ for inexact 6-mer and 7-mer motifs starting at nucleotides 12–18) (Figure 4D), this was a similar enrichment to that seen for canonical sites (Figure S5). These results support similar binding for noncanonical and canonical sites with complementarity to the 5′ end of the miRNA and frequent supplementary pairing to the 3′ end of the miRNA.

Since canonical miRNA target sites are flanked with sequences containing a high AU nucleotide content (Grimson et al., 2007; Nielsen et al., 2007), we examined AU content in noncanonical sites (Figure 4E). Consistent with previous studies, we found that sequences flanking AGO-bound miR-155 seed matches displayed higher AU content than unbound miR-155 seed matches and 3′ UTRs. Regions around noncanonical sites had higher AU content than 3′ UTR sequences or unbound miR-155 sites and in this regard were indistinguishable from AGO-bound canonical miR-155 sites.

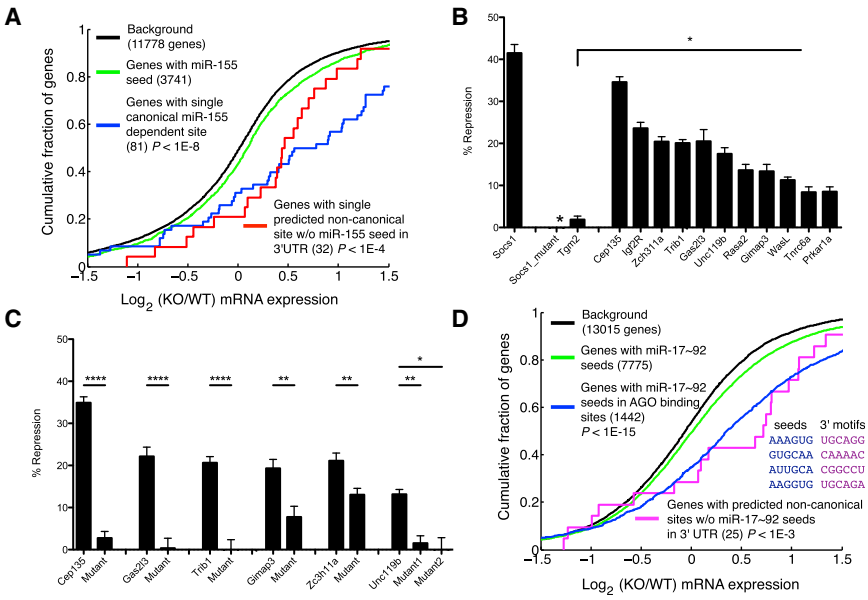

Figure 5. Gene Regulation by Noncanonical Sites

(A) Gene expression differences in miR-155-sufficient and -deficient T cells assessed by microarray. Expression is plotted for canonical targets and noncanonical targets without seed matches in the 3′ UTR.

(B) Repression of 3′ UTRs with noncanonical target sites by miR-155 assessed in luciferase reporter assays. Percent repression is the reduction in luciferase activity observed upon miR-155 overexpression relative to the luciferase activity observed with control miRNA overexpression. Socs1, a canonical target, the Socs1 miR-155 site mutant, and Tgm2 were used as positive and negative controls, respectively.

(C) Repression of luciferase reporter expression for constructs with and without mutations in the predicted noncanonical sites. Mutations are shown in Figure 3B.

(D) Gene expression differences from microarray data (Mu et al., 2009) of canonical targets and noncanonical targets that lacked miR-17~92 seed matches anywhere in the 3′ UTR in wild-type and miR-17~92 cluster-deficient B cell lymphoma cells.

Predicted noncanonical targets contain AGO binding sites with a single mismatch from miR-17~92 seed matches and an exact match to a 3′ motif.

In (B) and (C), mean ± SEM is plotted. *p < 0.05; **p < 0.01; ****p < 10^{-4}. See also Figure S6.

Noncanonical Targeting Is Associated with Moderate Regulation of Gene Expression by miR-155

Our results showed that miR-155 facilitated AGO binding at sites with inexact complementarity to the miR-155 seed. To assess the effect of these seed-like noncanonical sites on gene regulation, we examined targets with a single miR-155 dependent noncanonical site containing a motif with up to one mismatch from positions 1–6 or 2–7 of the miR-155 seed. To conservatively estimate the effect of these sites on gene expression we removed genes with a miR-155 seed match in the 3′ UTR. This set of genes was significantly regulated by miR-155 in activated T cells ($p < 10^{-4}$) (Figure 5A). However, these noncanonical targets were less regulated than genes containing a single canonical site and transcripts were not strongly regulated (<2-fold) by a noncanonical target site alone. The regulation of noncanonical targets was confirmed by comparing gene expression of these predicted noncanonical targets to the expression of genes associated with randomly chosen AGO-bound sites; this permutation test was also significant ($p < 0.05$). Together, these data suggest that noncanonical targeting alone can lead to modest regulation of gene expression.

To test whether miR-155 directly regulates gene expression through binding to noncanonical sites we evaluated the repression of many predicted noncanonical targets using luciferase reporter assays. We generated luciferase reporters containing target sites in their native 3′ UTR context (at least 450 nt of the 3′ UTR was used) and examined repression by miR-155 overexpressed in HEK293T cells (Figure 5B and Figure S6). Most noncanonical targets were clearly regulated by miR-155. One 3′ UTR (*Tgm2*) with an inexact seed, but without miR-155-dependent AGO binding, was also tested and showed no miR-155-dependent repression. Consistent with the moderate gene expression changes revealed by our global analysis, the noncanonical sites conferred less repression than the canonical target site in the 3′ UTR of the *Socs1* gene.

To test whether miR-155 mediated regulation depends on the noncanonical targets sites predicted by AGO dCLIP, we mutated these sites in a subset of luciferase reporter constructs (Figure 5C). In most cases, we made mutations at four nucleotides in regions with complementarity to the miRNA seed (Figure 3B). In one case, where we predicted contribution of 3′ interactions to miR-155 binding, we also mutated the corresponding 3′ site (Figure 3B). Mutations of the sites significantly reduced repression by miR-155. These experiments demonstrated that miR-155 binding to inexact seed sites can downregulate gene expression.

Prediction of Canonical and Noncanonical miRNA Targets Based on Gene Expression and AGO Binding Analyses

In addition to a genetically controlled transcriptome-wide identification of miR-155 targets, the AGO dCLIP data set enables analysis of target interactions with other miRNAs expressed in activated T cells (see Table S1). Thus, we investigated whether our data sets were predictive of canonical and noncanonical gene regulation by other endogenous miRNAs. Like miR-155, the miR-17~92 cluster is oncogenic (He et al., 2005), is overexpressed in human malignancies (He et al., 2005; Volinia et al., 2006), and regulates differentiation and survival of T and B cells (Jiang et al., 2011; Ventura et al., 2008; Xiao et al., 2008). We used previously published differential gene expression data from B cell lymphoma cells expressing or lacking the miR-17~92 cluster (Mu et al., 2009). Using this data set, we improved upon seed based predictions by filtering for miR-17~92 seed

Table 1. GO Enrichment Analysis

miRNA	Immune Process	Targets
miR-155	Negative regulation of B cell proliferation	BTLA, INPP5D, RC3H1
miR-155	Lymphocyte homeostasis	AHR, BCL2, CASP3, HIF1A, MEF2C, PMAIP1, SKIL
miR-21	Alpha-beta T cell differentiation	BCL11B, BCL2, SATB1, STAT6, TCF7
miR-21	Thymus development	BCL11B, BCL2, BCL2L11, CCNB2, CITED2, JARID2
miR-146	Enucleate erythrocyte differentiation	ID2, SP1, SP3
miR-146	Positive regulation of Th1 differentiation	CCR7, SOCS5
miR-17∼92	Embryonic hemopoiesis	GATA3, HIF1A, MLL1, RUNX1, TGFBR2
miR-17∼92	Negative regulation of T cell proliferation	BTLA, CBLB, CD274, IL2RA, ITCH, PDCD1LG2, RC3H1

The targets of miRNAs defined by seed matches in AGO CLIP binding sites in T cells were queried for enrichment in Gene Ontology immune processes. All functions with $p < 0.005$ using a hypergeometric test are listed. See also Figure S7.

matches in AGO binding sites (Figure 5D), demonstrating the utility of our data set for canonical miRNA target identification for other miRNAs and in other cellular contexts. We also observed moderate induction of genes with inexact complementarity to the miR-17∼92 seed (positions 1–6 or 2–7) and exact complementarity to positions 15–20 within AGO binding sites. Importantly, these results were unaffected by exclusion of genes containing miR-17∼92 seed matches anywhere in the 3′ UTR (Figure 5D). The success of our analysis of miR-17∼92 regulation of canonical and noncanonical sites was particularly remarkable considering that we used AGO binding sites identified in activated T cells and the miR-17∼92-dependent gene expression changes were measured in transformed B cells.

Analysis of miRNA Function in the Immune System

Since our data set provides the most complete and specific list of miRNA targets generated in the immune system, we checked whether targets of individual miRNAs present in activated T cells were enriched for specific immunological functions. Using Gene Ontology enrichment analysis, we found multiple functions enriched within the targets of miRNAs expressed in our data set (Table 1). Several functions predicted by this analysis have been confirmed; for example, miR-146a is necessary for preventing a T-helper 1 cell-driven autoimmunity (Lu et al., 2010), and miR-17∼92 overexpression leads to dysregulated T cell expansion and autoimmunity (Xiao et al., 2008). This analysis would fail unless miRNAs exert their effect through multiple targets. It therefore supports the idea that miRNAs are acting on multiple targets to affect a given function.

Based on GO analysis, which implicated miR-155 in lymphocyte homeostasis, we hypothesized that miR-155 contributes to proliferation of T cells. We examined the expansion of WT and 155KO T cells cotransferred into lymphopenic mice and found that 155KO T cells were outcompeted by WT counterparts (data not shown). This observation was in agreement with an established role for miR-155 in homeostasis of regulatory T cells, a specialized T cell lineage that expresses high levels of miR-155 (Lu et al., 2009). This analysis demonstrated the power of high-throughput miRNA target discovery for understanding miRNA dependent phenotypes.

Since we identified both the canonical and noncanonical targets of miR-155, we also explored the relationships between these targets (Figure S7). We identified several gene networks in which multiple components are targeted by miR-155. Together, these data support the hypothesis that miRNAs exert biological function through targeting of multiple functionally related genes.

DISCUSSION

The analysis of miR-155-dependent AGO binding sites in activated primary T cells provides a transcriptome-wide perspective of a miRNA's targets in an endogenous context. miR-155-AGO complexes are bound to over 300 canonical sites containing a perfect 6- to 8-mer seed in the 3′ UTR and this group of genes is strongly regulated by miR-155.

No miR-155 seeds were observed in ∼40% of miR-155-dependent AGO binding sites, and the majority of these sites contain inexact seed matches, which are associated with weaker regulation. Several rules for noncanonical sites have been described, notably for bulge sites and centered sites (Chi et al., 2012; Shin et al., 2010). Surprisingly, neither bulge sites nor centered sites were found among the miR-155 noncanonical sites. While centered sites are potent regulators of gene expression, they are relatively rare, with an average of several functional sites per miRNA (Shin et al., 2010)—so it was not surprising that they were not observed in our data set. In contrast, bulge sites are relatively common, accounting for up to one-quarter of all targets for some miRNAs (Chi et al., 2012); however, miR-155 appears to lack binding to this type of site.

Despite the modest level of regulation associated with noncanonical sites, these sites could play important biological roles. First, modest regulation of many targets may lead to important biological consequences—although there are not yet experimental systems for studying the effects of numerous moderate perturbations in gene expression. In addition, combinations of canonical and noncanonical sites may afford a wide spectrum of regulation of gene expression. Second, recent work suggested that miRNA binding sites on endogenous transcripts can compete for miRNA-AGO complexes and thereby upregulate other genes (Cesana et al., 2011; Jeyapalan et al., 2011; Karreth et al., 2011; Lee et al., 2009; Poliseno et al., 2010; Sumazin et al., 2011; Tay et al., 2011). Third, noncanonical sites may serve as an evolutionary midpoint for stronger canonical miRNA targeting. We therefore examined whether orthologous human 3′ UTR sequences of our predicted noncanonical targets were enriched for miR-155 seed matches. We found a modest enrichment ($p < 0.05$; hypergeometric test) for canonical motifs in human 3′ UTRs, suggesting that noncanonical targets may be an evolutionary midpoint. We also examined conservation using alignments of multiple species (Figure S8), which again suggested modest conservation of noncanonical sites.

As mentioned above, recent work suggested a model in which RNAs compete for miRNA-AGO complexes and reduce repression of other RNAs bearing sites for the same miRNAs (Cesana et al., 2011; Jeyapalan et al., 2011; Karreth et al., 2011; Lee et al., 2009; Poliseno et al., 2010; Sumazin et al., 2011; Tay et al., 2011). In this study, we found greater than 500 binding sites for miR-155 in a defined T cell lineage. The most-highly bound site, which occurs in a mitochondrial genome encoded RNA, accounts for ~20% of miR-155-dependent AGO binding. The most-highly bound site transcribed from the nuclear genome accounts for less than 5% of miR-155-dependent AGO binding. In total, only eight sites individually account for >1% of miR-155 dependent AGO binding. This suggests that at endogenous transcript levels very few transcripts bind a given miRNA-AGO complex at high enough levels to substantially influence the amount of free complex. Although data supporting competing endogenous RNAs focused on transcripts that share multiple miRNA binding sites, it seems unlikely that a transcript that altered the free pool of multiple miRNAs by <1% would significantly affect regulation of other targets. Therefore, we propose that if the competing endogenous transcript hypothesis is correct, then (1) very few endogenous transcripts bind sufficient miRNA-AGO complexes to alter targeting of other transcripts or (2) there is an as yet undescribed mechanism by which specific subsets of targets compete for restricted pools of miRNA-AGO complexes.

In summary, AGO dCLIP revealed that noncanonical AGO binding sites are a significant component of miRNA targeting, although they generally exert mild effects on gene regulation. We expect that differential CLIP-based techniques will facilitate further identification of functionally relevant noncanonical miRNA targets. It appears that similar to variations in transcription factor binding motifs, there is a spectrum of sequence motifs bound by RISC complexes loaded with a given miRNA and that these variations to the binding sites afford a continuum of miRNA-dependent regulation of gene expression.

EXPERIMENTAL PROCEDURES

dCLIP Website

Accessible binding maps for all 3′ UTRs are located at http://cbio.mskcc.org/leslielab/clipseq/.

Differential HITS-CLIP

$CD4^+$ T cells were harvested from WT and 155KO mice described elsewhere (Thai et al., 2007). All animal studies were performed in accordance with institutional guidelines. T cells were activated by culturing in the presence of CD3 and CD28 antibodies for 4 days at 37°C, 5% CO_2. Twelve HITS-CLIP libraries were constructed for both the activated WT and 155KO CD4+ cells, six with each 3′ linker sequence, which enabled statistical modeling of linker-induced biases. The libraries were constructed as described by Chi et al. (2009), with the following modifications. First, AGO immunoprecipitation was performed with a polyclonal antibody generated against an Argonaute 2 N-terminal peptide (O'Carroll et al., 2007). Second, so that contamination between libraries could be reduced, two different 3′ linker sequences were used, and reverse transcription (RT) was performed with primers that distinguish between the 3′ linkers. This permitted selective amplification of libraries. Third, the RT primers contained index tags, which enabled multiplex sequencing of libraries in a single sequencing lane. Fourth, for improvement of library complexity, the entire complementary DNA (cDNA) pool from each replicate was amplified in the presence of SYBR green dye with a real-time thermocycler so that amplification could be stopped near the end of the linear phase. Finally, random barcodes in the RT primer were used to distinguish between more frequently cloned regions and fragments preferentially amplified by PCR. We constructed libraries with barcodes 6 nt in length to extend the previous dynamic range of the assay. Sequencing was done on an Illumina GA2x as SE36 reads with an 11 nt index read to sequence the index and degenerate barcode.

Gene Expression Analysis

Cells were isolated and cultured as discussed above for 3 days. Cells were resuspended in Trizol and RNA was isolated according to manufacturer instructions. cDNA libraries were amplified and hybridized to Affymetrix MOE 430A 2.0 chips.

Computational and Bioinformatics Analyses

We constructed a 3′ UTR database for the mouse genome by identifying the longest annotated 3′ UTR for each gene in RefSeq or Ensembl. The annotated coding region sequence (CDS) of each gene was selected from the same transcript. The 3′ ends of reads were trimmed until the base quality score was >20. Reads that aligned uniquely to the mouse genome (with up to one mismatch) were mapped. Reads that mapped to the same genomic position and contained the same barcode were collapsed to a single read to reduce PCR bias. We also weighted read counts by normalizing to the library size aligned to the 3′ UTR database. mRNA expression data was mean centered and scaled to unit variance.

Luciferase Assays

HEK293T cells were cultured at 7×10^4 cells/well in a 24-well plate 1 day prior to transfection. psiCheck-2 vector (Promega) containing 3′ UTR regions were cotransfected with miR-155-expressing or control miR-146a-expressing pMDH-PGK-EGFP plasmids with Fugene 6 (Roche) in duplicate. Cells were harvested 18 hr later and luciferase activity was assayed using the Dual-Luciferase Reporter Assay System (Promega). Renilla Luciferase (bearing the cloned 3′ UTR) activity was normalized to Firefly Luciferase activity. Results from duplicate wells were averaged, and multiple ($n \geq 4$) independent experiments were pooled. Differences in repression across wild-type constructs was assessed with a one-way ANOVA followed by pairwise tests between the Tgm2-negative control and targets, adjusting for multiple comparisons with Dunnett's criterion. Differences in repression between mutant and wild-type constructs were assessed with paired t tests (Prism, GraphPad Software).

ACCESSION NUMBERS

The GEO accession number for the microarray and dCLIP data generated for this paper is GSE41288.

SUPPLEMENTAL INFORMATION

Supplemental Information includes Supplemental Experimental Procedures, eight figures, and three tables and can be found with this article online at http://dx.doi.org/10.1016/j.molcel.2012.10.002.

ACKNOWLEDGMENTS

We thank E.B. Conn Gantman and A. Mele for help with HITS-CLIP, C. Lee for assistance with sequencing, A. Tarakhovsky for the AGO2 antibody, and L.-F. Lu and A. Arvey for helpful discussions. This work was supported by NIH MSTP grant GM07739 (G.B.L.), and NIH grant R37 AI034206 (A.Y.R.). A.Y.R and R.B.D are investigators with the Howard Hughes Medical Institute.

Received: May 1, 2012
Revised: August 19, 2012
Accepted: October 2, 2012
Published online: November 8, 2012

REFERENCES

Ambros, V. (2004). The functions of animal microRNAs. Nature *431*, 350–355.

Bartel, D.P. (2004). MicroRNAs: genomics, biogenesis, mechanism, and function. Cell *116*, 281–297.

Bartel, D.P. (2009). MicroRNAs: target recognition and regulatory functions. Cell *136*, 215–233.

Betel, D., Koppal, A., Agius, P., Sander, C., and Leslie, C. (2010). Comprehensive modeling of microRNA targets predicts functional non-conserved and non-canonical sites. Genome Biol. *11*, R90.

Bolisetty, M.T., Dy, G., Tam, W., and Beemon, K.L. (2009). Reticuloendotheliosis virus strain T induces miR-155, which targets JARID2 and promotes cell survival. J. Virol. *83*, 12009–12017.

Brennecke, J., Stark, A., Russell, R.B., and Cohen, S.M. (2005). Principles of microRNA-target recognition. PLoS Biol. *3*, e85.

Cesana, M., Cacchiarelli, D., Legnini, I., Santini, T., Sthandier, O., Chinappi, M., Tramontano, A., and Bozzoni, I. (2011). A long noncoding RNA controls muscle differentiation by functioning as a competing endogenous RNA. Cell *147*, 358–369.

Chi, S.W., Zang, J.B., Mele, A., and Darnell, R.B. (2009). Argonaute HITS-CLIP decodes microRNA-mRNA interaction maps. Nature *460*, 479–486.

Chi, S.W., Hannon, G.J., and Darnell, R.B. (2012). An alternative mode of microRNA target recognition. Nat. Struct. Mol. Biol. *19*, 321–327.

Costinean, S., Zanesi, N., Pekarsky, Y., Tili, E., Volinia, S., Heerema, N., and Croce, C.M. (2006). Pre-B cell proliferation and lymphoblastic leukemia/high-grade lymphoma in E(mu)-miR155 transgenic mice. Proc. Natl. Acad. Sci. USA *103*, 7024–7029.

Costinean, S., Sandhu, S.K., Pedersen, I.M., Tili, E., Trotta, R., Perrotti, D., Ciarlariello, D., Neviani, P., Harb, J., Kauffman, L.R., et al. (2009). Src homology 2 domain-containing inositol-5-phosphatase and CCAAT enhancer-binding protein beta are targeted by miR-155 in B cells of Emicro-MiR-155 transgenic mice. Blood *114*, 1374–1382.

Didiano, D., and Hobert, O. (2006). Perfect seed pairing is not a generally reliable predictor for miRNA-target interactions. Nat. Struct. Mol. Biol. *13*, 849–851.

Doench, J.G., and Sharp, P.A. (2004). Specificity of microRNA target selection in translational repression. Genes Dev. *18*, 504–511.

Eis, P.S., Tam, W., Sun, L., Chadburn, A., Li, Z., Gomez, M.F., Lund, E., and Dahlberg, J.E. (2005). Accumulation of miR-155 and BIC RNA in human B cell lymphomas. Proc. Natl. Acad. Sci. USA *102*, 3627–3632.

Ender, C., Krek, A., Friedländer, M.R., Beitzinger, M., Weinmann, L., Chen, W., Pfeffer, S., Rajewsky, N., and Meister, G. (2008). A human snoRNA with microRNA-like functions. Mol. Cell *32*, 519–528.

Fang, Z., and Rajewsky, N. (2011). The impact of miRNA target sites in coding sequences and in 3'UTRs. PLoS ONE *6*, e18067.

Forman, J.J., Legesse-Miller, A., and Coller, H.A. (2008). A search for conserved sequences in coding regions reveals that the let-7 microRNA targets Dicer within its coding sequence. Proc. Natl. Acad. Sci. USA *105*, 14879–14884.

Gottwein, E., Corcoran, D.L., Mukherjee, N., Skalsky, R.L., Hafner, M., Nusbaum, J.D., Shamulailatpam, P., Love, C.L., Dave, S.S., Tuschl, T., et al. (2011). Viral microRNA targetome of KSHV-infected primary effusion lymphoma cell lines. Cell Host Microbe *10*, 515–526.

Grimson, A., Farh, K.K., Johnston, W.K., Garrett-Engele, P., Lim, L.P., and Bartel, D.P. (2007). MicroRNA targeting specificity in mammals: determinants beyond seed pairing. Mol. Cell *27*, 91–105.

Gu, S., Jin, L., Zhang, F., Sarnow, P., and Kay, M.A. (2009). Biological basis for restriction of microRNA targets to the 3′ untranslated region in mammalian mRNAs. Nat. Struct. Mol. Biol. *16*, 144–150.

Hafner, M., Landthaler, M., Burger, L., Khorshid, M., Hausser, J., Berninger, P., Rothballer, A., Ascano, M., Jr., Jungkamp, A.C., Munschauer, M., et al. (2010). Transcriptome-wide identification of RNA-binding protein and microRNA target sites by PAR-CLIP. Cell *141*, 129–141.

He, L., Thomson, J.M., Hemann, M.T., Hernando-Monge, E., Mu, D., Goodson, S., Powers, S., Cordon-Cardo, C., Lowe, S.W., Hannon, G.J., and Hammond, S.M. (2005). A microRNA polycistron as a potential human oncogene. Nature *435*, 828–833.

Jeyapalan, Z., Deng, Z., Shatseva, T., Fang, L., He, C., and Yang, B.B. (2011). Expression of CD44 3′-untranslated region regulates endogenous microRNA functions in tumorigenesis and angiogenesis. Nucleic Acids Res. *39*, 3026–3041.

Jiang, S., Li, C., Olive, V., Lykken, E., Feng, F., Sevilla, J., Wan, Y., He, L., and Li, Q.J. (2011). Molecular dissection of the miR-17-92 cluster's critical dual roles in promoting Th1 responses and preventing inducible Treg differentiation. Blood *118*, 5487–5497.

Karreth, F.A., Tay, Y., Perna, D., Ala, U., Tan, S.M., Rust, A.G., DeNicola, G., Webster, K.A., Weiss, D., Perez-Mancera, P.A., et al. (2011). In vivo identification of tumor- suppressive PTEN ceRNAs in an oncogenic BRAF-induced mouse model of melanoma. Cell *147*, 382–395.

Kluiver, J., Poppema, S., de Jong, D., Blokzijl, T., Harms, G., Jacobs, S., Kroesen, B.J., and van den Berg, A. (2005). BIC and miR-155 are highly expressed in Hodgkin, primary mediastinal and diffuse large B cell lymphomas. J. Pathol. *207*, 243–249.

Lal, A., Navarro, F., Maher, C.A., Maliszewski, L.E., Yan, N., O'Day, E., Chowdhury, D., Dykxhoorn, D.M., Tsai, P., Hofmann, O., et al. (2009). miR-24 Inhibits cell proliferation by targeting E2F2, MYC, and other cell-cycle genes via binding to "seedless" 3'UTR microRNA recognition elements. Mol. Cell *35*, 610–625.

Lee, D.Y., Shatseva, T., Jeyapalan, Z., Du, W.W., Deng, Z., and Yang, B.B. (2009). A 3′-untranslated region (3'UTR) induces organ adhesion by regulating miR-199a* functions. PLoS ONE *4*, e4527.

Leung, A.K., Young, A.G., Bhutkar, A., Zheng, G.X., Bosson, A.D., Nielsen, C.B., and Sharp, P.A. (2011). Genome-wide identification of Ago2 binding sites from mouse embryonic stem cells with and without mature microRNAs. Nat. Struct. Mol. Biol. *18*, 237–244.

Levati, L., Pagani, E., Romani, S., Castiglia, D., Piccinni, E., Covaciu, C., Caporaso, P., Bondanza, S., Antonetti, F.R., Bonmassar, E., et al. (2011). MicroRNA-155 targets the SKI gene in human melanoma cell lines. Pigment Cell Melanoma Res *24*, 538–550.

Lewis, B.P., Shih, I.H., Jones-Rhoades, M.W., Bartel, D.P., and Burge, C.B. (2003). Prediction of mammalian microRNA targets. Cell *115*, 787–798.

Lewis, B.P., Burge, C.B., and Bartel, D.P. (2005). Conserved seed pairing, often flanked by adenosines, indicates that thousands of human genes are microRNA targets. Cell *120*, 15–20.

Lim, L.P., Lau, N.C., Garrett-Engele, P., Grimson, A., Schelter, J.M., Castle, J., Bartel, D.P., Linsley, P.S., and Johnson, J.M. (2005). Microarray analysis shows that some microRNAs downregulate large numbers of target mRNAs. Nature *433*, 769–773.

Lu, L.F., Thai, T.H., Calado, D.P., Chaudhry, A., Kubo, M., Tanaka, K., Loeb, G.B., Lee, H., Yoshimura, A., Rajewsky, K., and Rudensky, A.Y. (2009). Foxp3-dependent microRNA155 confers competitive fitness to regulatory T cells by targeting SOCS1 protein. Immunity *30*, 80–91.

Lu, L.F., Boldin, M.P., Chaudhry, A., Lin, L.L., Taganov, K.D., Hanada, T., Yoshimura, A., Baltimore, D., and Rudensky, A.Y. (2010). Function of miR-146a in controlling Treg cell-mediated regulation of Th1 responses. Cell *142*, 914–929.

Metzler, M., Wilda, M., Busch, K., Viehmann, S., and Borkhardt, A. (2004). High expression of precursor microRNA-155/BIC RNA in children with Burkitt lymphoma. Genes Chromosomes Cancer *39*, 167–169.

Mu, P., Han, Y.C., Betel, D., Yao, E., Squatrito, M., Ogrodowski, P., de Stanchina, E., D'Andrea, A., Sander, C., and Ventura, A. (2009). Genetic dissection of the miR-17∼92 cluster of microRNAs in Myc-induced B-cell lymphomas. Genes Dev. *23*, 2806–2811.

Nielsen, C.B., Shomron, N., Sandberg, R., Hornstein, E., Kitzman, J., and Burge, C.B. (2007). Determinants of targeting by endogenous and exogenous microRNAs and siRNAs. RNA *13*, 1894–1910.

O'Carroll, D., Mecklenbrauker, I., Das, P.P., Santana, A., Koenig, U., Enright, A.J., Miska, E.A., and Tarakhovsky, A. (2007). A Slicer-independent role for Argonaute 2 in hematopoiesis and the microRNA pathway. Genes Dev. *21*, 1999–2004.

O'Connell, R.M., Rao, D.S., Chaudhuri, A.A., Boldin, M.P., Taganov, K.D., Nicoll, J., Paquette, R.L., and Baltimore, D. (2008). Sustained expression of microRNA-155 in hematopoietic stem cells causes a myeloproliferative disorder. J. Exp. Med. *205*, 585–594.

O'Connell, R.M., Chaudhuri, A.A., Rao, D.S., and Baltimore, D. (2009). Inositol phosphatase SHIP1 is a primary target of miR-155. Proc. Natl. Acad. Sci. USA *106*, 7113–7118.

Poliseno, L., Salmena, L., Zhang, J., Carver, B., Haveman, W.J., and Pandolfi, P.P. (2010). A coding-independent function of gene and pseudogene mRNAs regulates tumour biology. Nature *465*, 1033–1038.

Rai, D., Kim, S.W., McKeller, M.R., Dahia, P.L., and Aguiar, R.C. (2010). Targeting of SMAD5 links microRNA-155 to the TGF-beta pathway and lymphomagenesis. Proc. Natl. Acad. Sci. USA *107*, 3111–3116.

Rodriguez, A., Vigorito, E., Clare, S., Warren, M.V., Couttet, P., Soond, D.R., van Dongen, S., Grocock, R.J., Das, P.P., Miska, E.A., et al. (2007). Requirement of bic/microRNA-155 for normal immune function. Science *316*, 608–611.

Saraiya, A.A., and Wang, C.C. (2008). snoRNA, a novel precursor of microRNA in Giardia lamblia. PLoS Pathog. *4*, e1000224.

Schnall-Levin, M., Rissland, O.S., Johnston, W.K., Perrimon, N., Bartel, D.P., and Berger, B. (2011). Unusually effective microRNA targeting within repeat-rich coding regions of mammalian mRNAs. Genome Res. *21*, 1395–1403.

Shin, C., Nam, J.W., Farh, K.K., Chiang, H.R., Shkumatava, A., and Bartel, D.P. (2010). Expanding the microRNA targeting code: functional sites with centered pairing. Mol. Cell *38*, 789–802.

Skalsky, R.L., Corcoran, D.L., Gottwein, E., Frank, C.L., Kang, D., Hafner, M., Nusbaum, J.D., Feederle, R., Delecluse, H.J., Luftig, M.A., et al. (2012). The viral and cellular microRNA targetome in lymphoblastoid cell lines. PLoS Pathog. *8*, e1002484.

Sumazin, P., Yang, X., Chiu, H.S., Chung, W.J., Iyer, A., Llobet-Navas, D., Rajbhandari, P., Bansal, M., Guarnieri, P., Silva, J., and Califano, A. (2011). An extensive microRNA-mediated network of RNA-RNA interactions regulates established oncogenic pathways in glioblastoma. Cell *147*, 370–381.

Taft, R.J., Glazov, E.A., Lassmann, T., Hayashizaki, Y., Carninci, P., and Mattick, J.S. (2009). Small RNAs derived from snoRNAs. RNA *15*, 1233–1240.

Tay, Y., Kats, L., Salmena, L., Weiss, D., Tan, S.M., Ala, U., Karreth, F., Poliseno, L., Provero, P., Di Cunto, F., et al. (2011). Coding-independent regulation of the tumor suppressor PTEN by competing endogenous mRNAs. Cell *147*, 344–357.

Thai, T.H., Calado, D.P., Casola, S., Ansel, K.M., Xiao, C., Xue, Y., Murphy, A., Frendewey, D., Valenzuela, D., Kutok, J.L., et al. (2007). Regulation of the germinal center response by microRNA-155. Science *316*, 604–608.

Vella, M.C., Choi, E.Y., Lin, S.Y., Reinert, K., and Slack, F.J. (2004). The C. elegans microRNA let-7 binds to imperfect let-7 complementary sites from the lin-41 3'UTR. Genes Dev. *18*, 132–137.

Ventura, A., Young, A.G., Winslow, M.M., Lintault, L., Meissner, A., Erkeland, S.J., Newman, J., Bronson, R.T., Crowley, D., Stone, J.R., et al. (2008). Targeted deletion reveals essential and overlapping functions of the miR-17 through 92 family of miRNA clusters. Cell *132*, 875–886.

Vigorito, E., Perks, K.L., Abreu-Goodger, C., Bunting, S., Xiang, Z., Kohlhaas, S., Das, P.P., Miska, E.A., Rodriguez, A., Bradley, A., et al. (2007). microRNA-155 regulates the generation of immunoglobulin class-switched plasma cells. Immunity *27*, 847–859.

Vo, N.K., Dalton, R.P., Liu, N., Olson, E.N., and Goodman, R.H. (2010). Affinity purification of microRNA-133a with the cardiac transcription factor, Hand2. Proc. Natl. Acad. Sci. USA *107*, 19231–19236.

Volinia, S., Calin, G.A., Liu, C.G., Ambs, S., Cimmino, A., Petrocca, F., Visone, R., Iorio, M., Roldo, C., Ferracin, M., et al. (2006). A microRNA expression signature of human solid tumors defines cancer gene targets. Proc. Natl. Acad. Sci. USA *103*, 2257–2261.

Wang, H.Q., Yu, X.D., Liu, Z.H., Cheng, X., Samartzis, D., Jia, L.T., Wu, S.X., Huang, J., Chen, J., and Luo, Z.J. (2011). Deregulated miR-155 promotes Fas-mediated apoptosis in human intervertebral disc degeneration by targeting FADD and caspase-3. J. Pathol. *225*, 232–242.

Xiao, C., Srinivasan, L., Calado, D.P., Patterson, H.C., Zhang, B., Wang, J., Henderson, J.M., Kutok, J.L., and Rajewsky, K. (2008). Lymphoproliferative disease and autoimmunity in mice with increased miR-17-92 expression in lymphocytes. Nat. Immunol. *9*, 405–414.

Zhang, C., and Darnell, R.B. (2011). Mapping in vivo protein-RNA interactions at single-nucleotide resolution from HITS-CLIP data. Nat. Biotechnol. *29*, 607–614.

Zisoulis, D.G., Lovci, M.T., Wilbert, M.L., Hutt, K.R., Liang, T.Y., Pasquinelli, A.E., and Yeo, G.W. (2010). Comprehensive discovery of endogenous Argonaute binding sites in Caenorhabditis elegans. Nat. Struct. Mol. Biol. *17*, 173–179.